

# The Effect of Remote Donor Substituents on the Properties of Alkoxy and Amino Fischer Carbene Complexes of Tungsten

Nora-ann Weststrate,<sup>[a]</sup> Christopher Hassenrück,<sup>[b]</sup> Michael Linseis,<sup>[b]</sup> David C. Liles,<sup>[a]</sup> Simon Lotz,<sup>[a]</sup> Helmar Görls,<sup>[c]</sup> and Rainer F. Winter\*<sup>[b]</sup>

Dedicated to Prof. Wolfgang Kaim on the Occasion of his 70th Birthday

Tungsten Fischer ethoxy- and dimethylaminocarbene complexes  $[W\{C(X)(C_6H_4-4-R)(CO)_5\}]$  ( $X=OEt$ : series **a**; or  $X=NMe_2$ : series **b**) are synthesized from phenyl substrates containing remote tertiary amino substituents  $R'_2N$  with  $R'=Me$  (**2**), Ph (**3**) or  $C_6H_4Br-4$  (**4**). The  $\pi$ -delocalization and carbene-stabilizing effects of the distant tertiary amine donor substituent are investigated by NMR and IR spectroscopy, electrochemistry and quantum chemical calculations. A significant transfer of electron density from the remote 4- $R'_2N$  substituent to the carbene C

atom in the ethoxycarbene complexes is supported by NMR data and the solid-state structure of **2a**. This is strongly attenuated in the amino-substituted carbene complex **2c** and irrelevant in the dimethylaminocarbene complexes of series **b**, where the electron demand of the electrophilic carbene center is satisfied by the directly attached dimethylamino substituent. Quantum chemical calculations and IR spectroelectrochemistry on complexes **1a–4a** verify carbene-centered reductions and a ligand based oxidation of complex **2b**.

## Introduction

Fischer Carbene (FC) complexes with a heteroatom-substituted carbene ligand  $\{=C(X)R\}$  ( $X$ =heteroatom substituent,  $R$ =alkyl or aryl substituent) constitute powerful reagents in organic synthesis and readily participate in cycloaddition and template reactions,<sup>[1]</sup> with applications reaching to the labelling of sugars, nucleic acids or proteins.<sup>[2]</sup> In FC complexes, both the heteroatom donor  $X$  and the substituent  $R$  contribute to stabilizing the electrophilic carbene centre. These stabilizing effects are easily probed by virtue of the chemical shift of the carbene carbon atom in  $^{13}C$  NMR spectroscopy.<sup>[3]</sup> Table S1 of the Supporting Information (SI) provides an overview of

selected examples of FC complexes  $[W\{=C(X)R\}(CO)_5]$ , which cover a shift range of ca. 360 to 175 ppm, depending on the substituents  $R$  and  $X$ .

While the impact of a directly attached heteroatom substituent  $X$  has been scrutinized in great detail, the effect of a distant dialkyl- or diarylamino donor in phenyl-substituted FC ligands  $=C(X)(C_6H_4R-4)$  was only sporadically addressed.<sup>[1f]</sup> A distant nitrogen donor  $R'_2N$ , when in direct conjugation with the carbene carbon atom, can contribute to stabilizing the carbene centre via  $\pi$ -mesomeric effects (Figure 1).<sup>[4,5]</sup> In this study we pursue the aim of achieving a better understanding of the role of a distant  $R'_2N$  donor and to explore to which extent it may compete with the  $\alpha$ -heteroatom carbene donor substituent  $X$ . To these ends we investigate the electronic properties of appropriately substituted W carbene complexes through a combined analysis of their NMR, IR and structural data as obtained from X-ray crystallography, and their (spectro) electrochemical properties.

Konstanzer Online-Publikations-System (KOPS)

URL: <http://nbn-resolving.de/urn:nbn:de:bsz:352-2-123b4di74fxjd1>

## Results and Discussion

### Synthesis of the W(0) carbene complexes

The synthesis of the new W(0) carbene complexes  $[W\{=C(X)(C_6H_4-4-NR'_2)\}(CO)_5]$  with varying amine substituents  $R'$  and either an ethoxy (**2a–4a**) or a dimethylamino substituent  $X$  (**2b–4b**) follows the usual procedure of adding an appropriate amount of  $[W(CO)_6]$  to a cold ( $-78^\circ C$ ) solution of the respective lithiated arene to generate the corresponding acylates, followed by alkylation with  $Et_3O^+ BF_4^-$ .<sup>[6]</sup> The 4-dimethylamino derivatives **2b–4b** were generated from their ethoxy congeners by aminolysis with *in situ* generated dimethylamine (see

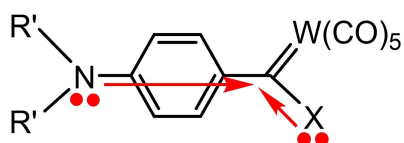
[a] N.-a. Weststrate, D. C. Liles, S. Lotz  
Department of Chemistry,  
University of Pretoria,  
Pretoria, 0002, South Africa

[b] C. Hassenrück, M. Linseis, R. F. Winter  
Fachbereich Chemie,  
Universität Konstanz,  
Konstanz, 78457, Germany  
E-mail: rainer.winter@uni-konstanz.de

[c] H. Görls  
Institut für Anorganische und Analytische Chemie,  
Friedrich-Schiller-Universität Jena,  
Jena, 07743, Germany

Supporting information for this article is available on the WWW under <https://doi.org/10.1002/zaac.202100081>

© 2021 The Authors. Zeitschrift für anorganische und allgemeine Chemie published by Wiley-VCH GmbH. This is an open access article under the terms of the Creative Commons Attribution Non-Commercial NoDerivs License, which permits use and distribution in any medium, provided the original work is properly cited, the use is non-commercial and no modifications or adaptations are made.



Remote vs adjacent carbene carbon atom stabilisation:  
X = OEt, NMe<sub>2</sub>; R' = alkyl, aryl

**Figure 1.** Competitive transfer of  $\pi$ -electron density from a remote amino and the  $\alpha$ -heteroatom substituent X towards a carbene-carbon metal carbonyl fragment.

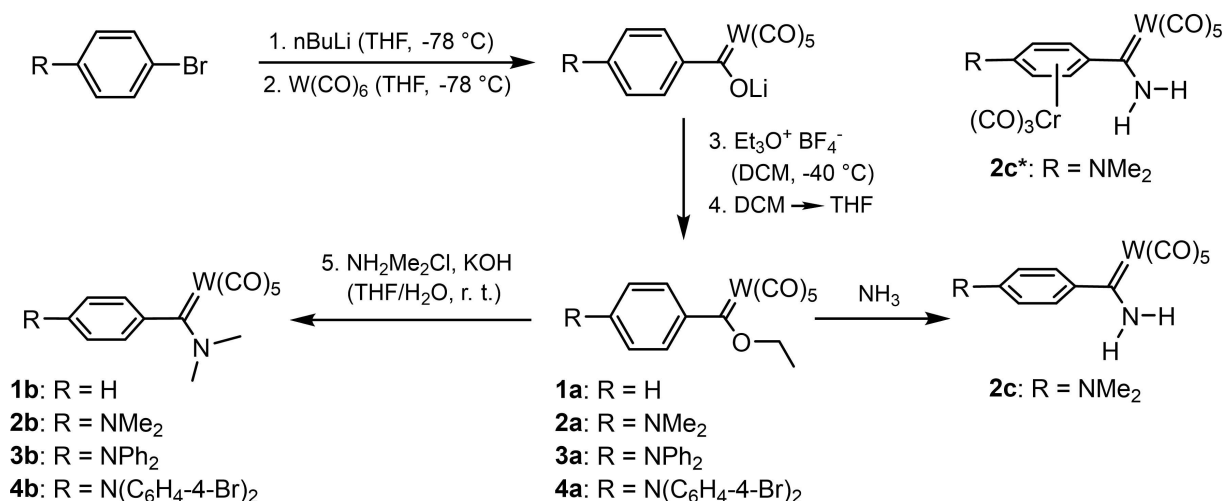
Scheme 1).<sup>[7]</sup> Complex  $[W\{C(NH_2)(C_6H_4-4-NMe_2)\}(CO)_5]$  (**2c**), where the aryl substituent acts as a  $\eta^6$ -arene ligand towards a  $\{Cr(CO)_3\}$  entity, was analogously made by bubbling ammonia through ether solutions of **2a**.<sup>[8]</sup> In order to avoid excessive decomposition, the synthesis of the heterobinuclear complex **2c\*** is best accomplished by the dropwise addition of a  $NH_3(g)$ -saturated ether solution to the ethoxycarbene precursor  $[W\{C(OEt)(\eta^6-C_6H_4-4-NMe_2)Cr(CO)_3\}(CO)_5]$  (**2a\***). Both these complexes were studied for structural comparison with **2b** and **2a**. The known complexes  $[W\{C(X)Ph\}(CO)_5]$  (X = OEt, NMe<sub>2</sub>) (**1a**, **1b**) lacking a 4-NR'<sub>2</sub> substituent at the phenyl ring, serve as points of comparison for complexes **2a–4a** and **2b–4b**.

### NMR Spectroscopy

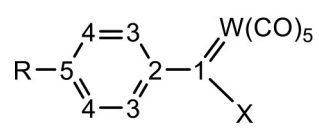
The <sup>1</sup>H and <sup>13</sup>C NMR spectra of all tungsten complexes are shown in Figures S1 to S10 in the Supporting Information. As follows from the compilation of the most pertinent data in Table 1, NMR spectra of the compounds reveal significant differences with respect to the presence and the nature of the 4-NR'<sub>2</sub> substituent at the phenyl ring. In the series of ethoxy complexes **1a** to **4a**, introducing a NR'<sub>2</sub> substituent in the 4-position of the phenyl ring shifts the resonance signals of the adjacent phenyl carbon atoms C4 and the attached protons H4 upfield while those of the remote carbon atoms C3 and protons H3 shift downfield (consult the header of Table 1 for the atomic

numbering scheme). This effect is most pronounced for complex **2a** with NMe<sub>2</sub> as the strongest donor of this series, where the differences  $\Delta\delta$  amount to 2.7/0.47 ppm for C3/H3, and to  $-18.1/-0.82$  ppm for C4/H4. The electron-donating effect of the NR'<sub>2</sub> substituent is even transmitted to the ethoxy substituent at the carbene carbon atom, where slight upfield shifts of 2.1 (CH<sub>2</sub>) and 0.07 (CH) ppm are observed. This effect is gradually attenuated in the NPh<sub>2</sub>- and the N(C<sub>6</sub>H<sub>4</sub>-4-Br)<sub>2</sub>-substituted complexes **3a** and **4a** as the electron-donating capabilities of the NR'<sub>2</sub> substituent decrease (for details see Table 1).

The <sup>13</sup>C NMR resonance of the carbene carbon atom of complex **2a** appears 21.3 ppm upfield of that in complex **1a**. This shift difference  $\Delta\delta$  amounts to a remarkable fraction of ca. one third of that of 63.8 ppm between the congeneric (phenyl)(ethoxy)- and (phenyl)(dimethylamino)-complexes **1a** and **1b**. Again, upfield shifts are attenuated in the NPh<sub>2</sub> and N(C<sub>6</sub>H<sub>4</sub>-4-Br)<sub>2</sub> derivatives **3a** and **4a**. A smaller shift difference  $\Delta\delta$  of  $-13.8$  ppm was previously observed for a related pair of thioether-substituted phenylcarbene complexes  $[W\{C(SC_2H_4OH)(C_6H_4-4-R)\}(CO)_5]$  (R = H, NMe<sub>2</sub>).<sup>[9]</sup> Varying the R' residues at the 4-NR'<sub>2</sub> substituent has however only minor effects on the positioning of the corresponding resonance signal in aminocarbene complexes **1b–4b**, which all group into a narrow range of 256.7 to 258.2 ppm. Obviously, the  $\alpha$ -nitrogen atom of an aminocarbene complex acts as such a strong  $\pi$ -electron donor towards the carbene carbon atom that the remote



**Scheme 1.** Synthesis of **1a–4a**, **1b–4b** and **2c**.

**Table 1.** Selected  $^1\text{H}$  NMR and  $^{13}\text{C}$  NMR chemical shifts  $\delta$  (ppm) in  $\text{CD}_2\text{Cl}_2$  and spectral assignments for complexes **1 a–4 a**, **1 b–4 b**, **2 c** and **2 c\***.


X = OEt (**a**), NMe<sub>2</sub> (**b**), NH<sub>2</sub> (**c**)  
**1**: R = H  
**2**: R = NMe<sub>2</sub>  
**3**: R = NPh<sub>2</sub>  
**4**: R = N{C<sub>6</sub>H<sub>4</sub>Br}<sub>2</sub>

$^1\text{H}/^{13}\text{C}$ X = OEt	1	2	3	4	5	CH <sub>2</sub> (OEt)	CH <sub>3</sub> (OEt)
<b>1 a</b>	-/320.5	-/155.9	7.56/132.0	7.47/128.5	7.47/126.6	5.06/81.0	1.71/15.2
<b>2 a</b>	-/299.2	-/154.9	8.03/134.7	6.65/110.4	-/140.9	4.99/78.9	1.64/13.3
<b>3 a</b>	-/305.8	-/151.5	7.84/132.8	6.88/125.9	-/145.5	5.02/79.7	1.65/15.2
<b>4 a</b>	-/308.4	-/152.0	7.80/131.6	6.94/118.4	-/147.2	5.04/80.1	1.67/15.2
X = NMe <sub>2</sub> ( <b>b</b> ) or NH <sub>2</sub> ( <b>c</b> ) <sup>[a]</sup>						NMe <sub>2</sub> /NH <sub>2</sub>	
<b>1 b</b>	-/256.7	-/153.8	6.80/128.8	7.42/119.4	7.18/126.6	3.93, 3.03/44.8	
<b>2 b</b>	-/258.2	-/149.4	6.74/122.3, 120.7	6.68/112.5, 111.3	-/143.5	3.89, 3.04/43.8, 39.5	
<b>3 b</b>	-/257.2	-/148.8	7.06/123.4	6.70/121.2	-/146.3	3.91, 3.14/44.9	
<b>4 b</b>	-/256.9	-/149.9	7.11/125.3	6.75/121.6	-/145.4	3.93, 3.16/44.8	
<b>2 c</b>	-/255.3	-/152.8	7.50/129.0	6.68/111.2	-/137.6	8.47, 8.05/40.1	
<b>2 c*</b> <sup>[b]</sup>	-/261.4	-/n. o	5.45/93.8, 92.1	4.74/71.9, 70.1	/n. o	8.93, 8.69/40.5, 39.1	

[a] Chemical shifts of the N(CH<sub>3</sub>) protons in complexes **1 b–4 b** and of the N(CH<sub>3</sub>) carbon atoms in complexes **2 b**, **2 c\*** differ due to restricted rotation around the C<sub>carbene</sub>-N bond. [b] Resonance signals of the phenyl carbon atoms are duplicated due to planar chirality.

nitrogen donor substituent 4-NR'<sub>2</sub> makes no detectable contribution to stabilizing the carbene centre. This seems to also hold true for the simple amine-substituted complex **2 c** and the closely related complex [W{C=NHMe(C<sub>6</sub>H<sub>4</sub>-4-Me)}(CO)<sub>5</sub>] (Table 1).<sup>[10]</sup> η<sup>6</sup>-Coordination of the phenyl substituent of **2 c** to a Cr(CO)<sub>3</sub> entity in **2 c\*** has the known effect of shifting the resonances of the phenyl carbon atoms and protons upfield by more than 35 ppm or ca. 2 ppm, respectively.<sup>[8a]</sup>

### X-ray Crystallography

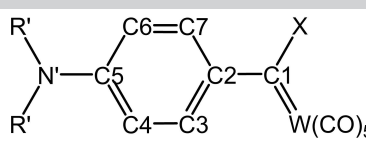
Single crystals of complexes **2 a**, **2 b**, **2 c**, **2 c\*** and **3 a** were obtained by careful layering of saturated solutions of the corresponding complexes in CH<sub>2</sub>Cl<sub>2</sub> with *n*-hexane and their solid-state structures were determined by single crystal X-ray diffraction. Tables S2 and S3 of the Supporting Information summarize relevant information on the data collection and refinement. The molecular structures of complexes **1 a**,<sup>[11]</sup> **4 a**<sup>[12]</sup> and of the complex [W{C(NHMe)(Ph)}(CO)<sub>5</sub>], the NHMe-substituted analog of complex **1 b** (denoted as **1 b**<sup>NHMe</sup> in Table 2), have been previously published and will be used for comparative purposes, along with that of complex **2 c\***. MERCURY<sup>[13]</sup> drawings of the molecular structures of **2 a**, **2 b**, **2 c** and **3 a** are displayed in Figure 2, Table 2 lists the most relevant bond lengths, bond angles and torsion angles.

Figure 3 displays the three most relevant resonance structures that can be conceived for a heteroatom-substituted tungsten FC complex. Electron donation from the lone pair at the heteroatom substituent X or the remote 4-NR'<sub>2</sub> substituent at the phenyl ring will increase the contributions of the zwitterionic resonance structures II and III with respect to I. Key

structural manifestations of the zwitterionic resonance structures (and their mutual competition) are a shortening of the C-X (II) or a shortening of the C<sub>ph</sub>-C<sub>carbene</sub> (C1-C2) and the N-C<sub>ph</sub> (N'-C5) bonds (see also the numbering scheme in the header of Table 2) as well as a quinoidal distortion of the phenylene ring (III). Both zwitterionic resonance structures will contribute to lengthening the W=C1 bond to the carbene atom. Such effects have been amply noted in the literature<sup>[5b,7a, 14]</sup> and are also manifest in the present series of complexes.

The data for the present set of complexes should also be compared to the [W{CPh<sub>2</sub>}(CO)<sub>5</sub>] benchmark system with its W-C1 bond length of 2.15(2) Å.<sup>[15]</sup> Further points of comparison are provided by the complexes [W{CN(allyl)CH<sub>2</sub>CH<sub>2</sub>N(allyl)}(CO)<sub>5</sub>] (W-C1 = 2.266(3) Å),<sup>[16]</sup> [W{CN(Et)CMeCMeN(Et)}(CO)<sub>5</sub>] (W-C1 = 2.275(8) Å) with an unsaturated NHC ligand,<sup>[14b]</sup> and the acyclic aminoxy carbene complex [W{C(OEt)N{C(CHPh)CH<sup>n</sup>Pr<sup>i</sup>Pr<sup>j</sup>}(CO)<sub>5</sub>] (W-C1 = 2.297(8) Å),<sup>[17]</sup> where steric congestion caused by the bulky amino substituent on the carbene carbon atom may also contribute to the bond lengthening.

On first comparing the 4-NR'<sub>2</sub>-substituted (phenyl)(ethoxy) carbene complexes of series **a** (**2 a–4 a**) with the parent phenyl complex **1 a**, we note a distinct elongation of the W-C1 and shortening of the C1-C2 bond in the former complexes as well as the signatures of a quinoidal distortion of the phenylene ring (Figure 4), all in line with a structurally relevant contribution of resonance form III. Similar observations were also made for the related *N,N*-diallyl and pyrrolinyl complexes, where the W-C1 and C1-C2 bond lengths are 2.233(9) or 2.245(3) and 1.468(11) or 1.454(3) Å, respectively.<sup>[5b]</sup> Another indication for the relevance of resonance structure III is the compressed C5-N bond of 1.358(3) Å or 1.378(4) Å in complexes **2 a** and **3 a**. The shortening of this bond becomes evident on comparison with

**Table 2.** Selected bond lengths (Å) and angles (°) of the single X-ray crystal structures of **1 a–4 a**, **2 b**, **2 c**, **2 c\***


	<b>1 a</b> <sup>[11b]</sup> X=OEt	<b>2 a</b> X=OEt	<b>3 a</b> X=OEt	<b>4 a</b> <sup>[12]</sup> X=OEt	<b>2 b</b> X=NMe <sub>2</sub>	<b>2 c</b> X=NH <sub>2</sub>	<b>2 c*</b> <sup>[a]</sup> X=NH <sub>2</sub>	<b>1 b</b> <sup>NHMe[7a]</sup> X=NHMe
<b>Bond lengths (Å)</b>								
N–C5	–	1.358(3)	1.378(4)	1.398(4)	1.379(4)	1.368(3)	1.345(3), 1.360(3)	–
C1–C2	1.496(5)	1.461(4)	1.472(4)	1.482(5)	1.504(4)	1.470(3)	1.485(3), 1.490(3)	1.484(29)
C1–X	1.310(4)	1.337(3)	1.325(3)	1.317(4)	1.303(4)	1.312(3)	1.305(3), 1.300(3)	1.299(26)
C1–W	2.201(3)	2.229(3)	2.235(3)	2.221(3)	2.251(3)	2.244(2)	2.213(2), 2.210(2)	2.186(22)
<b>Bond angles (°)</b>								
R'–N'–C5	–	121.3(3)	122.6(2)	119.6(3)	119.7(3)	121.3(2)	121.5(2), 120.3(2)	–
R'–N'–C5	–	120.5(2)	120.3(2)	123.9(3)	119.6(3)	120.5(2)	121.1(2), 120.3(2)	–
R'–N'–R'	–	118.2(2)	116.6(2)	116.6(3)	116.8(3)	118.0(2)	116.2(2), 116.2(2)	–
C2–C1–X	105.3(3)	106.5(2)	106.9(2)	106.0(3)	113.9(3)	112.6(2)	113.2(2), 112.9(2)	113.7(2)
C2–C1–W	124.5(2)	126.5(2)	126.6(2)	127.0(2)	116.9(2)	126.9(1)	124.6(2), 123.9(2)	121.9(2)
W–C1–X	130.1(3)	127.1(2)	126.5(2)	127.0(2)	129.1(2)	120.4(2)	122.1(2), 123.2(2)	124.3(2)
Me–N–Me	–	–	–	–	111.1(3)	–	–	–
Me–N–C1	–	–	–	–	122.9(3)	–	–	–
Me–N–C1	–	–	–	–	126.0(3)	–	–	–
<b>Torsion angles (°)</b>								
R'–N'–C5–C4	–	–0.4(4)	–3.8(4)	15.6(5)	15.9(5)	–6.5(4)	–4.4(4), –9.5(4)	–
W–C1–C2–C3	–41.0(5)	20.8(4)	2.0(4)	11.2(4)	–90.1(3)	37.5(3)	–32.8(3), –43.3(3)	74.6(2)
X–C1–C2–C7	–36.2(5)	16.2(4)	–1.3(4)	8.6(4)	–89.7(4)	33.1(3)	–29.3(3), –42.3(3)	78.9(2)
<b>Dihedral Angles (°)<sup>[b]</sup></b>								
Plane 1, Plane 2	39.0(2)	19.2(2)	2.4(1)	9.8(2)	89.6(2)	35.9(1)	31.9(1), 43.2(1)	77.4(2)
Plane 2, Plane 3	–	2.8(2)	8.5(1)	16.7(2)	5.2(2)	5.0(2)	1.3(2), 3.0(2)	–

[a] Data for the two independent molecules of **2 c\*** within the unit cell. [b] Plane 1: W,X,C1,C2 (4 atoms); Plane 2: C2 to C7 (6 atoms); Plane 3: C5,N,R',R' (4 atoms).

the value of 1.390(4) Å in *N,N*-dimethylaniline<sup>[18]</sup> and those of 1.408(7) to 1.427(7) Å for the four independent molecules within the unit cell of triphenylamine.<sup>[19]</sup> Moreover, the phenyl ring as well as the attached 4-NR'<sub>2</sub> substituent adopt a coplanar orientation with respect to the plane W, O, C1, C2 spanned by the carbene carbon atom, which is a structural prerequisite for mesomeric stabilization of the carbene centre by the remote amino substituent. As one might expect, the magnitude of these structural alterations with respect to the parent phenyl complex **1 a** are gradually attenuated as the electron-donating capabilities of the NR'<sub>2</sub> substituent decrease from **2 a** to **4 a**.

The effect of heteroatom substitution at the carbene centre becomes evident on comparing the structures of complexes **2 a**, **2 b** and **2 c**, which all have a 4-NMe<sub>2</sub>-substituent at the phenylene ring (see Figure 4 for an overlay of the structures of **2 a,b** and a comparison with the DFT/b3lyp/def2TZV calculated structures). The most conspicuous differences are a slight lengthening of the W–C1, the C1–C2, as well as of the N–C5 bonds in the order **2 a** < **2 c** < **2 b**. This ordering parallels that of increasing electron-donating capabilities of the heteroatom substituent X and indicates an increasing relevance of the resonance structure II at the expense of III. So, as X becomes a stronger donor, mesomeric stabilization of the electrophilic carbene centre by the electron-rich remote substituent at the

phenyl ring becomes secondary or even irrelevant. This is also borne out by the fact that all C–C bonds within the phenylene ring of **2 b** are equal within error margins. In the complexes of series **b**, the steric demands of the NMe<sub>2</sub> substituent render it impossible to put the nearby phenylene ring in the same plane. In this competition for carbene stabilization, the stronger NMe<sub>2</sub> donor wins. Hence, the 4-NMe<sub>2</sub>C<sub>6</sub>H<sub>5</sub> substituent of **2 b** is forced into an orthogonal orientation with respect to the carbene plane. This puts the phenylene π-system and the nitrogen lone-pair out of resonance with the empty p-orbital of the carbene carbon atom. Steric constraints are mitigated in the NH<sub>2</sub>-substituted complex **2 c**. Bond parameters and the orientation of the phenylene ring in complex **2 c** are therefore in between those of **2 a** and **2 b**. π-Coordination of the phenyl ring to the electron withdrawing {Cr(CO)<sub>3</sub>} fragment in **2 c\*** essentially “neutralizes” the electron donating capabilities of the remote 4-NMe<sub>2</sub> substituent such that the bond lengths C1–C2 and C1–W come close to those in phenyl-substituted **1 a**.

### Cyclic voltammetry

Most metal carbene complexes undergo an oxidation and a reduction process. Investigations on several series of carbene

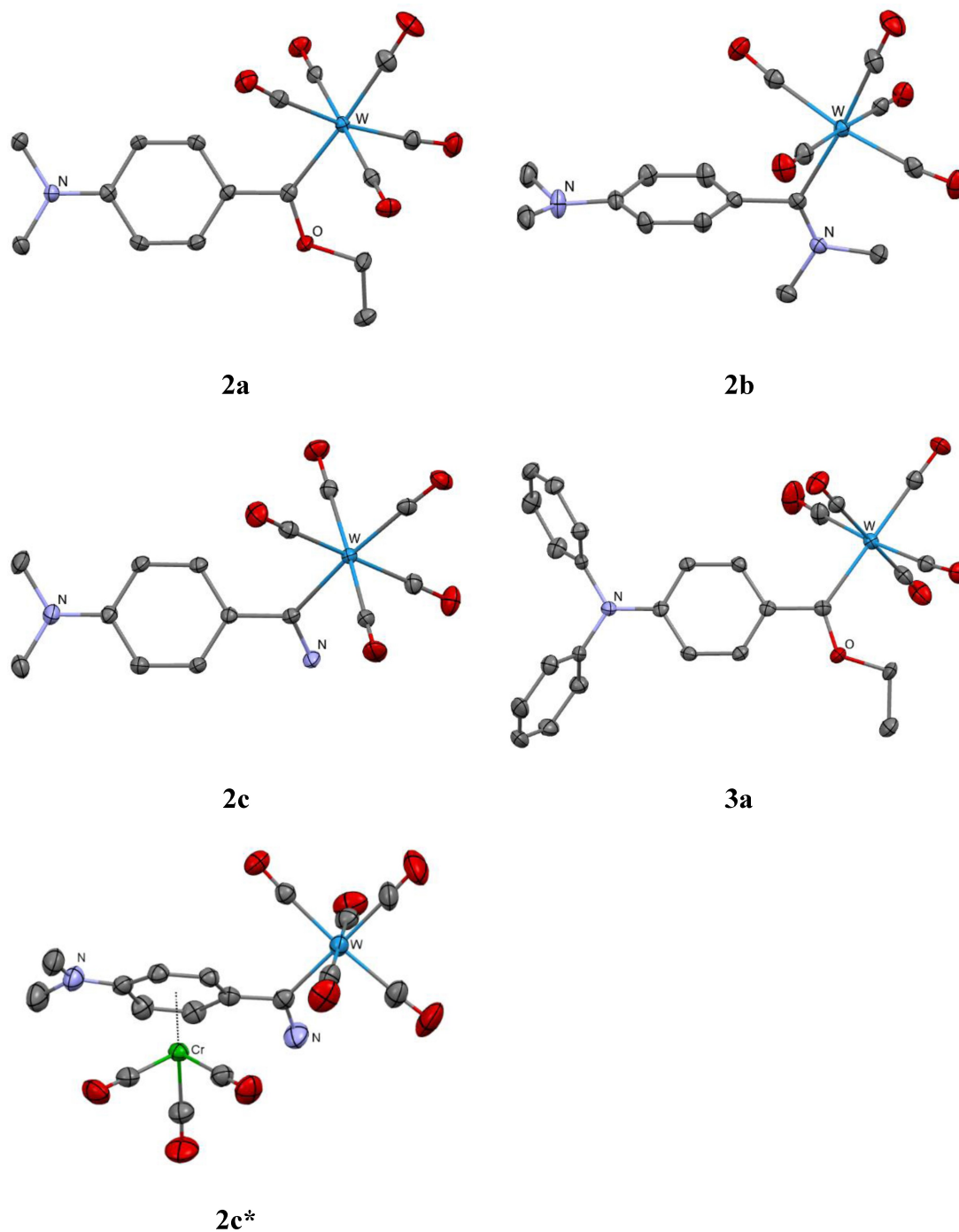


**Figure 2.** Solid state structures of complexes **2a** (top left), **2b** (top right), **2c** (middle left), **3a** (middle right) and **2c\*** (bottom left). In the *MERCURY*<sup>31</sup> drawings the ADP ellipsoids are set at a 50% probability level and hydrogen atoms are omitted for clarity reasons.

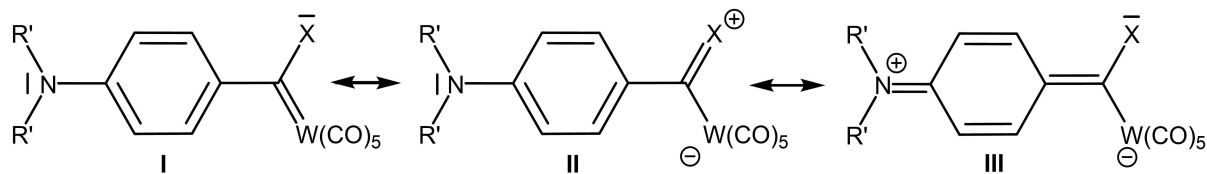


**Figure 3.** The most important resonance structures for the present carbene complexes.

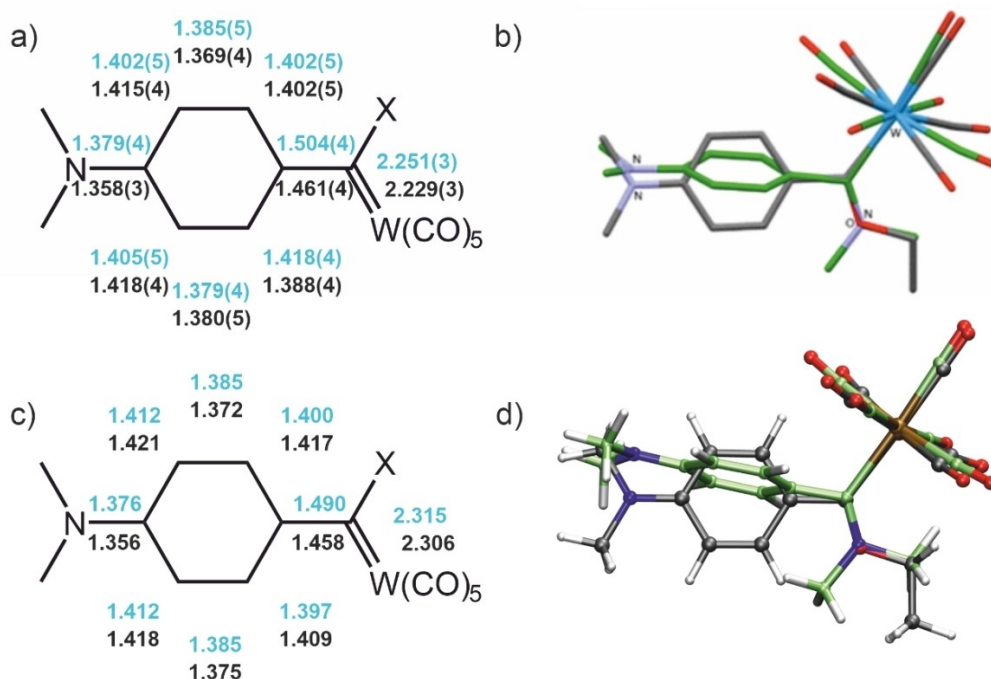


**Figure 4.** Comparison of relevant bond lengths (Å) from the experimental (X-ray) structure (a) and the DFT/b3lyp/def2TZVP calculated structure (c) of **2a** (black, X=OEt) and **2b** (blue, X=NMe<sub>2</sub>); overlay of the structures of **2a** (grey C atoms) and **2b** (green C atoms, for the experimental (b) and calculated structures (d)).

complexes indicated that the oxidation is generally more metal-based, while the reduction is strongly biased towards the carbene ligand.<sup>[20]</sup> Thus, variation of the 4-substituent R in aminocarbene complexes [Cr{C(NMe<sub>2</sub>)(C<sub>6</sub>H<sub>4</sub>-4-R)}(CO)<sub>5</sub>] (R = OMe, Me, H, Cl) was found to have a *ca.* fourfold higher impact on the reduction half-wave potential  $E_{1/2}^{\text{red}}$  than on the oxidation potential  $E_{1/2}^{\text{ox}}$  with a linear scaling of potential drifts with the substituents' Hammett  $\sigma_{\text{para}}$  parameters. Computed compositions of the frontier MOs of carbene complexes are in line with these assignments.<sup>[1e,20a-n]</sup>

The present series of complexes offer the opportunity to study the effects of introducing an even stronger electron donor 4-NR<sub>2</sub>' in the 4-position of a phenyl substituent and of more subtle alterations of the remote amine substituents R'. Cyclic voltammetry on the present complexes was conducted in the CH<sub>2</sub>Cl<sub>2</sub>/NBu<sub>4</sub>PF<sub>6</sub> (0.1 M) electrolyte. Representative voltammograms of the complexes are displayed in Figure 5, and Table 3 lists the derived potential values against the ferrocene/ferrocenium redox couple ( $E_{1/2}(\text{Cp}_2\text{Fe}^{0/+}) = 0$  mV).

Under the present conditions all ethoxycarbene complexes of series **a** are irreversibly oxidized but undergo a reversible one-electron reduction. Attachment of the 4-NR<sub>2</sub>' substituent to the phenyl ring introduces a second possible oxidation site (note that amino-substituted benzenes and, in particular, triaryl amines are themselves redox-active).<sup>[21]</sup> Hence, two oxidation processes are observed for **2a** and **4a**. The same would be expected for the simple diphenylamine congener **3a**. However, the associated radical cation of this complex is subject to rapid, more complex chemical follow-up processes which generate

**Table 3.** Oxidation and reduction half wave/peak potentials of **1a–4a** and **1b–4b** in CH<sub>2</sub>Cl<sub>2</sub>/0.1 M NBu<sub>4</sub>PF<sub>6</sub> at a scan rate of 100 mV/s

Complex	$E^{\text{ox}}/\text{V}$	$E^{\text{red}}/\text{V}$	Complex	$E^{\text{ox}}/\text{V}$	$E^{\text{red}}/\text{V}$
<b>1a</b>	0.695 <sup>[a]</sup>	−1.835	<b>1b</b> <sup>[b]</sup>	0.455 <sup>[a]</sup> , 1.180 <sup>[a]</sup> , 1.490 <sup>[a]</sup>	–
<b>2a</b>	0.405 <sup>[a]</sup> , 0.800 <sup>[a]</sup>	−2.030	<b>2b</b> <sup>[b]</sup>	0.085	–
<b>3a</b>	0.525 <sup>[a]</sup> , 0.840 <sup>[c]</sup> , 0.950 <sup>[c]</sup>	−1.919	<b>3b</b>	0.190 <sup>[a]</sup>	−2.35 <sup>[a]</sup>
<b>4a</b>	0.580 <sup>[a]</sup> , 0.890 <sup>[a]</sup>	−1.840	<b>4b</b> <sup>[b]</sup>	0.240	–

[a] Peak potential of a chemically irreversible redox process. [b] Reduction falls outside the solvent window. [c] Irreversible anodic processes of electroactive follow products generated upon the first oxidation.

further electroactive products showing up as smaller peaks anodic of that of the first oxidation (see Figure S13 of the Supporting Information). Such behaviour is reminiscent of unsubstituted triphenylamine itself.<sup>[22]</sup> We also note that replacement of the 4-NMe<sub>2</sub> substituent of **2a** by (4-Br-C<sub>6</sub>H<sub>4</sub>)<sub>2</sub>N in **4a** has a larger effect on the potential of the first than on that of the second oxidation. The chemical irreversibility of both anodic processes does, however, not allow for a clear assignment of the initial oxidation site (the metal ion or the aryl- or

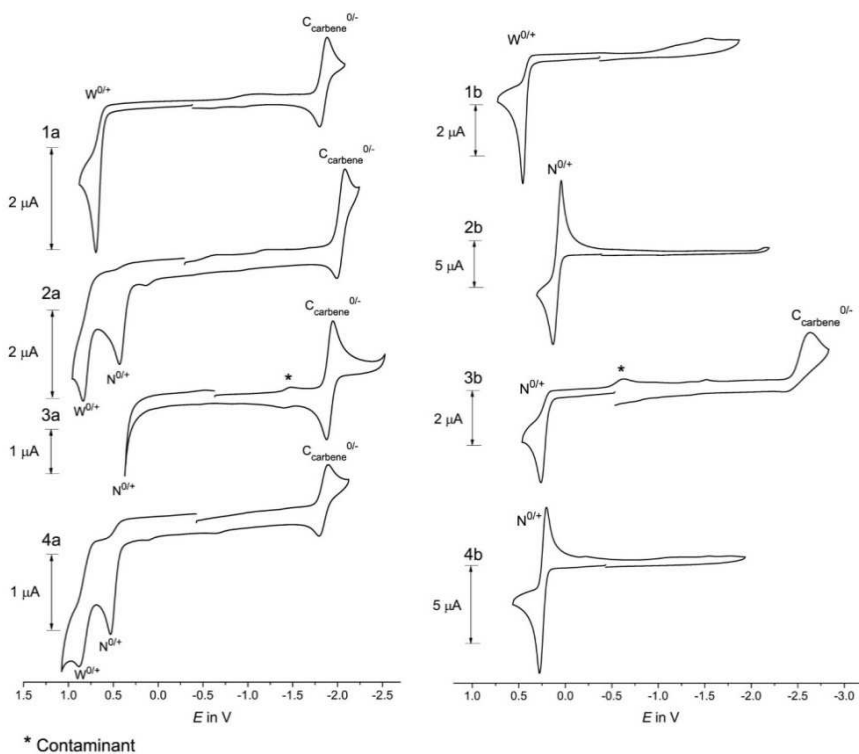


**Figure 5.** Cyclic voltammograms of complexes **1a,b** to **4a,b** in the  $\text{CH}_2\text{Cl}_2/0.1 \text{ M NBu}_4\text{PF}_6$  electrolyte at a  $100 \text{ mV/s}$  scan rate referenced against the  $\text{Cp}_2\text{Fe}^{0/+}$  redox couple.

triarylamine substituent) solely on the basis of the electrochemical data.

The aminocarbene complexes of series **b** oxidize at much less positive potentials than their analogous ethoxycarbene congeners. In the case of complexes **2b** and **4b**, the oxidation is chemically fully reversible even at low sweep rates (**2b**) or becoming so at sweep rates of  $\geq 400 \text{ mV/s}$  (**4b**). In contrast, no reduction wave was observed within the solvent window of the  $\text{CH}_2\text{Cl}_2/\text{NBu}_4\text{PF}_6$  electrolyte. The cathodic shift of the oxidation potential by  $> 300 \text{ mV}$  between congeners of the **a** and **b** series of complexes clearly surpasses that of  $80 \text{ mV}$  to  $170 \text{ mV}$  for comparable alkoxy- and dimethylaminocarbene complexes,<sup>[7b,20f,j,m,23]</sup> as it was particularly well documented for 2-furyl- or 2-thienyl-substituted derivatives.<sup>[20b,i,24]</sup> This argues for an unusually large contribution of the donor-substituted phenylene moiety at the carbene ligand to the oxidation process. The anodic shift of the peak potential  $E_p^{\text{ox}}$  of ca.  $0.05 \text{ V}$  for complex pairs **3a/4a** and **3b/4b**, which mirrors the electron-withdrawing effect of the two bromo substituents on the amine-appended phenyl ring, is not too dissimilar to that of  $0.03 \text{ V}$  to  $0.10 \text{ V}$  (depending on the solvent and the supporting electrolyte) for the corresponding triarylamines  $(\text{C}_6\text{H}_5)(\text{C}_6\text{H}_4\text{-4-Br})_2\text{N}$  and  $\text{Ph}_3\text{N}$ .<sup>[21a,d,25]</sup>

In seeking to gain further insight into the composition of the relevant frontier MOs and, by inference, the identity of the likely redox site for oxidation and reduction, we conducted quantum chemical studies on all complexes of series **a** and **b**. Their geometry-optimized structures agree well with exper-

imental ones. Contour plots of the relevant frontier MOs (HOMO, LUMO) of the complexes **1a–4a** and **1b–4b** are displayed in Figure 6 along with the differences in NBO-calculated charges of the individual fragments,  $\{\text{W}(\text{CO})_5\}$ ,  $\text{C}(\text{X})$ ,  $\text{C}_6\text{H}_4$  and  $4\text{-NR}'_2$ , upon oxidation or reduction (for listings of fragment NBO charges and their differences on oxidation and reduction see Tables S4 and S5 of the Supporting Information). Despite the different orientations of the  $4\text{-NR}'_2\text{-C}_6\text{H}_4$  plane to that defined by the carbene carbon atom and the attached W, X and  $\text{C}_{\text{ph}}$  atoms between complexes of series **a** and **b**, the HOMO of all complexes bearing a  $4\text{-NR}'_2$  substituent is delocalized over the donor-substituted phenylene ring and the  $\{\text{W}(\text{CO})_5\}$  moiety, but does not receive any significant contributions from the carbene carbon atom and the heteroatom substituent X. Based on these results, the first oxidation of the ethoxycarbene complexes cannot be adequately described as either metal- or ligand-based, but assumes a mixed character. The LUMO of the ethoxycarbene complexes is similarly delocalized, but receives higher contributions from the immediate carbene fragment  $\text{C}(\text{OEt})(\text{C}_6\text{H}_4)$  at the expense of the attached  $4\text{-NR}'_2$  substituent and the  $\{\text{W}(\text{CO})_5\}$  entity. This is further augmented in the aminocarbene complexes, where the contributions of the  $4\text{-NR}'_2$  substituent to the HOMO are increased, whereas those to the LUMO become almost nil.

Importantly, the compositions of the frontier MOs are not altered by one-electron oxidation. Hence, the contour diagrams of the energetically highest-lying singly occupied molecular orbital (SOMO) of the corresponding, one-electron oxidized

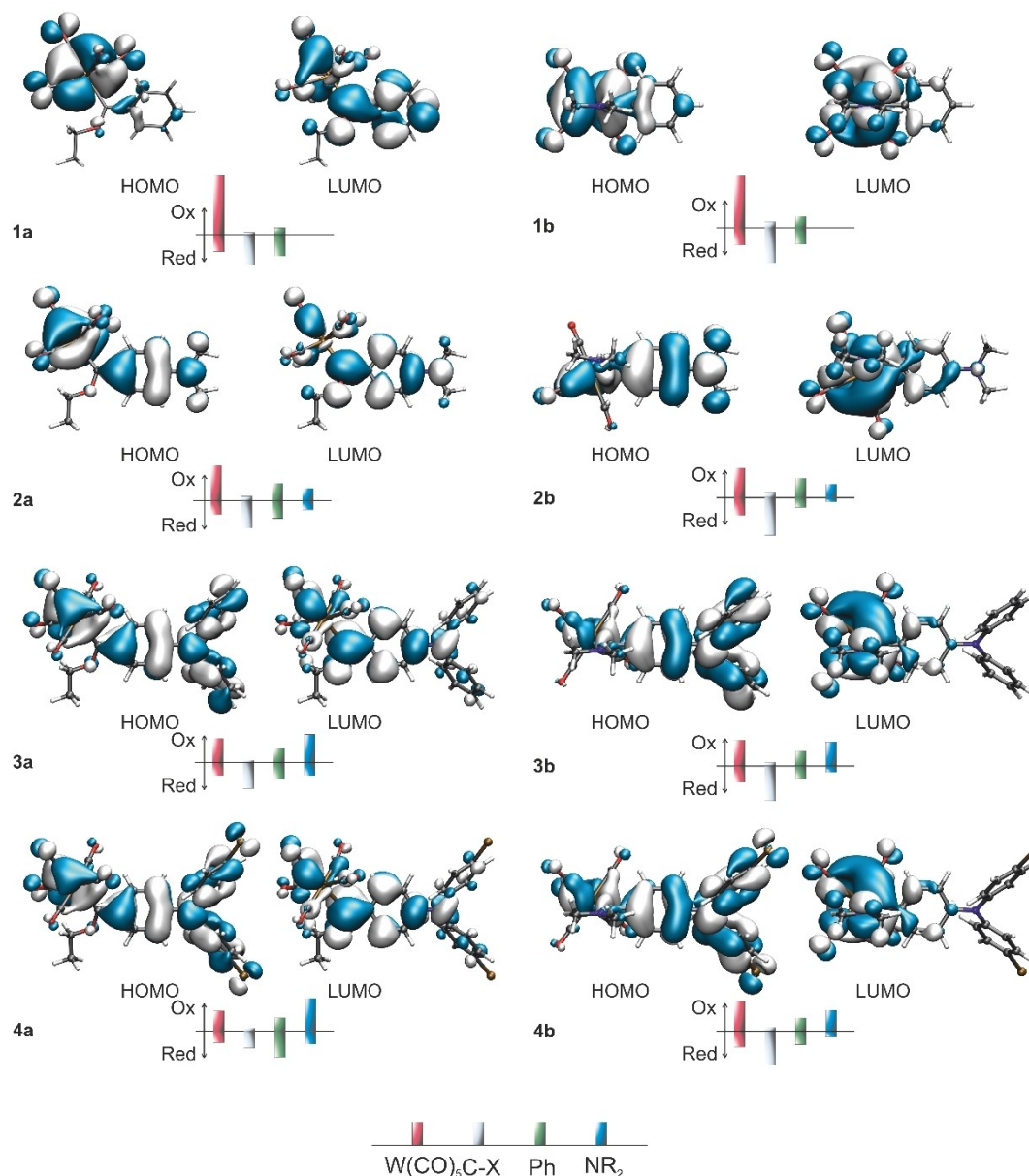


**Figure 6.** Contour plots of the calculated HOMO (left) and LUMO (right) of the neutral complexes **1 a–4 a** and differences in the NBO calculated atomic partial charges upon oxidation and reduction (see legend at the bottom).

cations match with those of the HOMO of the neutral congeners, while those of the associated one-electron reduced anions are largely identical to the LUMO of the complexes (see Figures S14 and S15 of the Supporting Information). The computed spin densities as shown in Figures S16 and S17 of the Supporting Information retrace the MO coefficients of the respective fragments.

Taken together, our calculations show that the remote 4-NR<sub>2</sub> substituent has a clear impact on the composition of the relevant frontier MOs in that the HOMO is directed away from the {W(CO)<sub>5</sub>} fragment towards the 4-NR<sub>2</sub>-C<sub>6</sub>H<sub>4</sub> substituent. This goes even to the point where the HOMO is dominated by the (tri)arylamine entity. *Vice versa*, our calculations also predict unusually large

contributions of the {W(CO)<sub>5</sub>} fragment to the reduction, particularly for the aminocarbene complexes of series **b**.

### IR Spectroscopy and IR Spectroelectrochemistry

The positions of the various  $\nu(\text{CO})$  bands of a {M(CO)<sub>5</sub>} fragment in complexes [M(CO)<sub>5</sub>(L)] are an excellent indicator of the electronic properties of a ligand L.<sup>[26]</sup> Moreover, band shifts on one-electron oxidation or reduction trace metal participation to the corresponding redox process with an expected shift of *ca.* 90–150 cm<sup>-1</sup> for a dominantly metal-centred process.<sup>[20a,27]</sup> Table 4 lists the energies of the characteristic CO bands for every complex. The red shift of all bands in the aminocarbene



**Table 4.** IR data for the  $\nu(\text{CO})$  bands of complexes **1 a–4 a** and **2 b–4 b** in THF at RT and for reduced species **1 a<sup>−</sup>–4 a<sup>−</sup>** as well as oxidized **2 b<sup>+</sup>** in THF/1.5 M NBu<sub>4</sub>PF<sub>6</sub>

	$\tilde{\nu}(\text{CO})$ ( $\text{W}(\text{CO})_5$ ) in $\text{cm}^{-1}$			
	$A_1^{(1)}$	$B_1$	E	$A_1^{(2)}$
<b>1 a</b>	2068	1983 (w)	1940 (vs)	n.o.
<b>1 a<sup>−</sup></b>	2040	n.o.*	1900	1844
<b>2 a</b>	2060	1973 (w)	1929 (vs)	n. o.
<b>2 a<sup>−</sup></b>	2035	1940	1896	1852
<b>3 a</b>	2063	1976 (w)	1933 (vs)	n.o.
<b>3 a<sup>−</sup></b>	2043	n. o.*	1900	1871
<b>4 a</b>	2064	1977 (w)	1934 (vs)	n. o.
<b>4 a<sup>−</sup></b>	2039	1938	1900	1864
<b>1 b</b>	2062	1968 (w)	1925 (vs)	1905 (sh)
<b>2 b</b>	2060	1968 (w)	1924 (vs)	1903 (sh)
<b>2 b<sup>+</sup></b>	2064	1972 (vw)	1928 (vs)	1910 (sh)
<b>3 b</b>	2060	1969 (w)	1925 (vs)	1906 (sh)
<b>4 b</b>	2060	1969 (w)	1925 (vs)	1904 (sh)

complexes as compared to their oxycarbene congeners is fully in line with the increased donor capabilities of the heteroatom substituent in the former and matches with earlier observations.<sup>[14a,c, 20f, m]</sup> When comparing the differently substituted ethoxycarbene complexes of series **a**, one notes that introducing a 4-NR'<sub>2</sub> donor to the phenylene substituent causes a red shift of all CO bands. The energies  $\tilde{\nu}_{\text{CO}}$  decrease in parallel with an increasing donor capability of NR'<sub>2</sub> as shown by the ordering **1 a** > **4 a** > **3 a** > **2 a**. For complexes of series **b**, however, no such effect is observed. This matches with our observations from <sup>13</sup>C NMR spectroscopy, implying that the C<sub>6</sub>H<sub>4</sub>-NR'<sub>2</sub> substituent does very little to stabilize the carbene centre.

The reversible reduction of the ethoxycarbene complexes allowed us to monitor the changes in the  $\nu(\text{CO})$  bands during this process by means of IR spectroelectrochemistry as an experimental probe for {W(CO)<sub>5</sub>} contribution to the reduction.

The results of such experiments on complex **2 a** are shown in the left-hand panel of Figure 8 while those for complexes **1 a**, **3 a** and **4 a** can be found as Figure S18 of the Supporting Information. A shift to lower wavenumbers of approximately 25  $\text{cm}^{-1}$  ( $A_1^{(1)}$ -band) to 40  $\text{cm}^{-1}$  (E-band) is observed for every complex. This is far less than the shift of 90  $\text{cm}^{-1}$  to 115  $\text{cm}^{-1}$  observed for metal-centred oxidations of other metal carbene complexes,<sup>[20o,27b]</sup> but compares well with shifts of 13  $\text{cm}^{-1}$  to 29  $\text{cm}^{-1}$  observed for the reduction of the complex [Re {C(OEt)(TTh)}Br(CO)<sub>4</sub>] (TTh = 2,3-*b*-thiothiophenediyl) with a likewise delocalized LUMO.<sup>[7b]</sup> The chemical reversibility of the oxidation wave of the aminocarbene complex **2 b** allowed us to also monitor the CO band shifts during this process. A graphical account of the outcome of this experiment is shown in the right-hand panel of Figure 7. The CO bands experience an only minor displacement of ca. 4  $\text{cm}^{-1}$  to higher energies, thus clearly identifying the 4-NR'<sub>2</sub>-C<sub>6</sub>H<sub>4</sub> substituent as the oxidation site.

## Conclusions

In the present work we have explored to what extent a 4-NR'<sub>2</sub> substituent at the phenyl residue of a carbene ligand (= C(X)(C<sub>6</sub>H<sub>4</sub>-4-NR'<sub>2</sub>)) contributes to stabilizing the electrophilic carbene carbon atom in {W(CO)<sub>5</sub>} Fischer Carbene complexes. To these ends we have varied the heteroatom substituent X from ethoxy to dimethylamino as well as the electron donating capabilities of the 4-NR'<sub>2</sub> substituent (R' = Me, Ph, 4-BrC<sub>6</sub>H<sub>5</sub>). We have scrutinized the NMR and IR spectroscopic and the electrochemical properties of the complexes as well as the structural data of several representatives and compared them among each other and with those of their simple phenyl congeners [W {CX(Ph)}(CO)<sub>5</sub>]. Based on these results we conclude that electron donation from the 4-NR'<sub>2</sub>-C<sub>6</sub>H<sub>4</sub> substituent plays an important

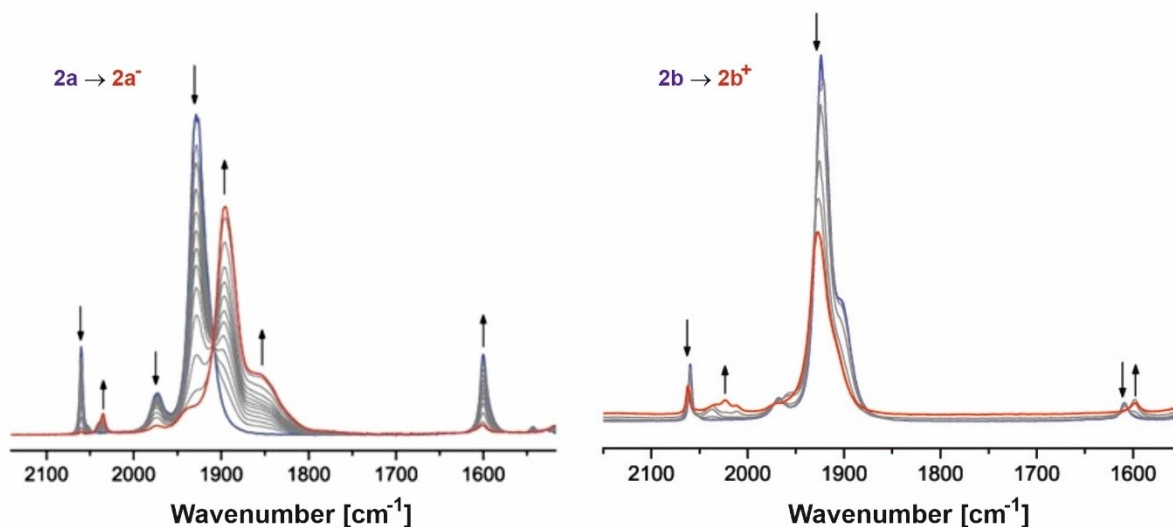


**Figure 7.** IR spectroscopic changes in the carbonyl region during the reduction of complex **2 a** (left) and the oxidation of complex **2 b** (right) in CH<sub>2</sub>Cl<sub>2</sub> /0.1 M NBu<sub>4</sub>PF<sub>6</sub>.

role in the oxycarbene complexes, but is wholly irrelevant in the aminocarbene complexes. The remote, conjugated 4-NR<sub>2</sub> donor substituent can thus be employed to fine-tune the electronic properties of oxycarbene complexes as it can provide additional electron density to stabilize the carbene carbon atom. The presence of the 4-NR<sub>2</sub> donor has also a strong influence on the composition of the relevant frontier MOs, thus directing the first oxidation of the aminocarbene complexes away from the metal carbene entity to the (tri)arylamine constituent of complexes **3b**, **4b**.

## Experimental

### Material and Methods

Standard Schlenk techniques, performed under an atmosphere of Ar or N<sub>2</sub>, were used for synthesis. THF and hexane were distilled over sodium metal, while CH<sub>2</sub>Cl<sub>2</sub> was distilled over CaH<sub>2</sub>. All other reagents were used as received from commercial suppliers. Et<sub>3</sub>O<sup>+</sup> BF<sub>4</sub><sup>-</sup> was synthesised according to the published procedure by Meerwein.<sup>[6]</sup> Aminolysis with dimethylamine is achieved through an acid-base reaction between dimethylammonium chloride and sodium hydroxide in an aqueous environment.<sup>[7b]</sup> Silica gel 60 (particle size 0.0063–0.200 mm) was used as the stationary phase for all separations in column chromatography. NMR spectra were recorded on Bruker Ultrashield Plus 400 AVANCE 3 and Bruker Ultrashield 300 AVANCE 3 spectrometers using CD<sub>2</sub>Cl<sub>2</sub> as solvent at 25 °C. The NMR spectra were recorded for <sup>1</sup>H at 400.13 or 300.13 MHz and <sup>13</sup>C at 100.163 or 75.468 MHz. Chemical shifts were recorded in ppm, using the deuterated solvent signal as an internal reference (CD<sub>2</sub>Cl<sub>2</sub>: δH at 5.3400 and δC at 53.840 ppm). Figure 8 provides the atomic numbering and positional assignment of H and C atoms for the NMR spectra of the Synthesis section. Cyclic voltammetry was performed in an air-tight one compartment cell with a Pt working electrode (1.6 mm diameter from BAS), a coiled Pt counter electrode and a coiled Ag wire as pseudo reference electrode. Before measurements, the working electrode was polished with 1 μm and 0.25 μm diamond pastes (Buehler-Wirtz). NBu<sub>4</sub>PF<sub>6</sub> (0.25 mM) was used as the supporting electrolyte in THF. Referencing was done by adding ferrocene, decamethylferrocene (Cp\*<sub>2</sub>Fe) or cobaltocenium hexafluorophosphate as an internal standard to the analyte solution after all data of interest had been acquired. Representative sets of scans were repeated in the presence of the added standard. Final referencing was done against the ferrocene/ferrocenium (Cp<sub>2</sub>Fe<sup>0/+</sup>) couple with E<sub>1/2</sub> (Cp\*<sub>2</sub>Fe<sup>0/+</sup>) = –540 mV vs. Cp<sub>2</sub>Fe<sup>0/+</sup> and E<sub>1/2</sub> (Cp<sub>2</sub>Co<sup>0/+</sup>) = –1330 mV vs. Cp<sub>2</sub>Fe<sup>0/+</sup> using THF/NBu<sub>4</sub>PF<sub>6</sub> as the supporting electrolyte. Voltammetric data were acquired with a computer-controlled BASi CV50 potentiostat. FT-IR spectra were recorded on a Thermo is 10 instrument. A

custom-built optically transparent thin layer electrolysis cell equipped with CaF<sub>2</sub> windows, Pt mesh as working and counter electrodes and a thin Ag sheet as the pseudo-reference electrode following the design of Hartl and co-workers was used for spectroelectrochemistry.<sup>[28]</sup>

Density functional theory (DFT) calculations were performed on the full model complexes using the Gaussian 09 Rev. D program packages.<sup>[29]</sup> Open shell systems were calculated by the unrestricted Kohn-Sham approach (UKS). Geometry optimization followed by vibrational analysis was performed in solvent media. Solvent effects were described by the polarizable continuum model (PCM) with standard parameters for THF.<sup>[30]</sup> Within Gaussian 09 calculations the valence polarised triple-ζ basis sets (def2-TZVP)<sup>[31]</sup> were employed for all atoms together with the b3lyp functional.<sup>[31c,32]</sup> The GaussSum program package was used to analyze the results,<sup>[33]</sup> while the visualization of the results was performed with the Avogadro program package.<sup>[34]</sup> Graphical representations of molecular orbitals were generated with the help of GNU Parallel<sup>[35]</sup> and plotted using the vmd program package<sup>[36]</sup> in combination with POV-Ray.<sup>[37]</sup>

### Crystallography

The intensity data for compounds **2a**, **2b**, were collected on a Nonius KappaCCD diffractometer using graphite-monochromated Mo-Kα radiation (λ = 0.71073 Å). Data were corrected for Lorentz and polarization effects; absorption was taken into account on a semi-empirical basis using multiple-scans.<sup>[38]</sup>

The structures were solved by direct methods using SHELXS<sup>[39]</sup> and refined by full-matrix least squares techniques against Fo<sup>2</sup> using SHELXL-97.<sup>[40]</sup> The hydrogen atoms of compound **2a** were located by difference Fourier synthesis and refined isotropically. The hydrogen atoms of all other complexes were included at calculated positions with fixed thermal parameters.

The intensity data for compounds **2c**, **2c**\*(SI) and **3a** were collected on a Bruker D8 Venture kappa-geometry diffractometer, fitted with twin IμS sources and a Photon-100 CMOS detector, using Mo-Kα radiation (λ = 0.71073 Å) and Bruker APEX3<sup>[41]</sup> control software. The data were processed using Bruker SAINT and were corrected for absorption by the multi-scan method, and scaled using Bruker SADABS (Bruker, 2014). The structures were solved by a dual-space algorithm using Bruker SHELXTS and refined using Bruker SHELXTL and SHELXL-2014/7.<sup>[40]</sup> The N–H hydrogen atom positions in **2c** were refined, all other hydrogen atoms were included in calculated positions and allowed to ride on the positions of the carbon atoms to which they are bonded. The ADP of every hydrogen atom was set at 1.2× (1.5× for the methyl hydrogen atoms) the equivalent isotropic ADP of the associated carbon atom.

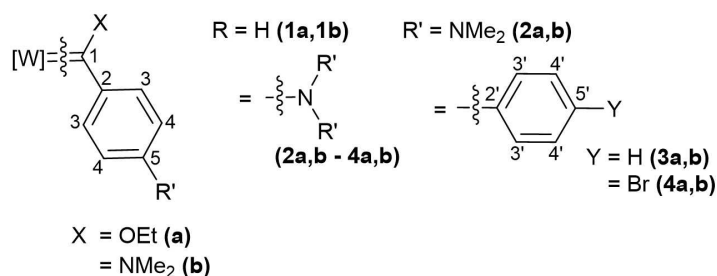


Figure 8. NMR positional assignments for complexes **1a–4a**, **1b–4b**, **2c** and **2c**\*.

## Synthesis

## Synthesis and characterisation of ethoxy- and aminocarbene complexes of tungsten (1a–4a, 1b–4b, 2c and 2c\*)

**1a:** Bromobenzene (1.65 mL, 10.0 mmol) was dissolved in 30 mL of THF and cooled to  $-78^{\circ}\text{C}$ .  $n\text{-BuLi}$  (7.50 mL, 12.0 mmol) was added to the cold solution while stirring and then  $[\text{W}(\text{CO})_6]$  (3.52 g, 10.0 mmol) was added. The reaction mixture was allowed to stir for 30 minutes at  $-70^{\circ}\text{C}$  followed by 30 minutes at room temperature. The solvent was removed under vacuum and the remaining residue was dissolved in  $\text{CH}_2\text{Cl}_2$ . The solution was cooled to  $-40^{\circ}\text{C}$  and  $\text{Et}_3\text{OBF}_4$  (1.90 g, 10.0 mmol), dissolved in  $\text{CH}_2\text{Cl}_2$ , was added to the cold reaction mixture. Then it was allowed to stir for 30 minutes at room temperature. The reaction mixture was passed through a silica plug and the orange product was isolated using silica column chromatography with *n*-hexane and  $\text{CH}_2\text{Cl}_2$  as solvents. Yield = 2.06 g (45.0%).  $\text{C}_{14}\text{H}_{16}\text{O}_6\text{W}$ .  $^1\text{H}$  NMR ( $\text{CD}_2\text{Cl}_2$ , 400 MHz)  $\delta = 7.56$  (d,  $^3J_{\text{HH}} = 8.4$  Hz, 2H, H3), 7.47 (m, 2H, H4), 7.47 (m, 1H, H5), 5.06 (q,  $^3J_{\text{HH}} = 7.1$  Hz, 2H,  $\text{H}_{\text{CH}_2}$ ), 1.71 ppm (t,  $^3J_{\text{HH}} = 7.1$  Hz, 3H,  $\text{H}_{\text{CH}_3}$ ).  $^{13}\text{C}$  NMR ( $\text{CD}_2\text{Cl}_2$ , 101 MHz)  $\delta = 320.5$  ( $^1J_{\text{WC}} = \text{n.o.}$ ,  $\text{C}_{\text{carb}}$ ), 204.4 ( $^1J_{\text{WC}} = \text{n.o.}$ ,  $\text{C}_{\text{W}(\text{CO})_5}$ , *trans*), 197.9 ( $^1J_{\text{WC}} = 64.2$  Hz,  $\text{C}_{\text{W}(\text{CO})_5}$ , *cis*), 155.9 (C2), 132.0 (C3), 128.5 (C4), 126.6 (C5), 81.0 ( $\text{C}_{\text{CH}_2}$ ), 15.2 ppm ( $\text{C}_{\text{CH}_3}$ ). ESI-MS (2.8 V, positive mode,  $m/z$ ): calcd for  $[\text{M}]^+$  458.0013; found 458.0387.

**2a:** The same synthesis procedure as for **1a** was followed, employing 4-bromo-*N,N*-dimethylaniline (3.00 g, 15.0 mmol),  $n\text{-BuLi}$  (9.38 mL, 15.0 mmol),  $\text{W}(\text{CO})_6$  (5.28 g, 15.0 mmol),  $\text{Et}_3\text{OBF}_4$  (2.85 g, 15.0 mmol). Yield = 2.87 g (38.2%).  $\text{C}_{16}\text{H}_{15}\text{O}_6\text{NW}$ .  $^1\text{H}$  NMR ( $\text{CD}_2\text{Cl}_2$ , 400 MHz)  $\delta = 8.03$  (d,  $^3J_{\text{HH}} = 9.3$  Hz, 2H, H3), 6.65 (d,  $^3J_{\text{HH}} = 9.3$  Hz, 2H, H4), 4.99 (q,  $^3J_{\text{HH}} = 7.0$  Hz, 2H,  $\text{H}_{\text{CH}_2}$ ), 3.11 (s, 6H,  $\text{NMe}_2$ ), 1.64 ppm (t,  $^3J_{\text{HH}} = 7.0$  Hz, 3H,  $\text{H}_{\text{CH}_3}$ ).  $^{13}\text{C}$  NMR ( $\text{CD}_2\text{Cl}_2$ , 101 MHz)  $\delta = 299.2$  ( $^1J_{\text{WC}} = 50.1$  Hz,  $\text{C}_{\text{carb}}$ ), 203.8 ( $^1J_{\text{WC}} = 60.2$  Hz,  $\text{C}_{\text{W}(\text{CO})_5}$ , *trans*), 199.7 ( $^1J_{\text{WC}} = 64.1$  Hz,  $\text{C}_{\text{W}(\text{CO})_5}$ , *cis*), 154.9 (C2), 140.9 (C5), 134.7 (C3), 110.4 (C4), 78.9 ( $\text{C}_{\text{CH}_2}$ ), 40.3 ( $\text{NMe}_2$ ), 13.3 ppm ( $\text{C}_{\text{CH}_3}$ ). ESI-MS (2.8 V, positive mode,  $m/z$ ): calcd for  $[\text{M} + \text{H}]^+$  502.0487; found 502.0453.

**3a:** The same synthesis procedure as for **1a** was followed using 4-bromotriphenylamine (3.24 g, 10.0 mmol),  $n\text{-BuLi}$  (6.60 mL, 10.0 mmol),  $\text{W}(\text{CO})_6$  (3.52 g, 10.0 mmol) and  $\text{Et}_3\text{OBF}_4$  (1.89 g, 10.0 mmol). Yield = 2.37 g (37.9%).  $\text{C}_{26}\text{H}_{19}\text{O}_6\text{NW}$ .  $^1\text{H}$  NMR ( $\text{CD}_2\text{Cl}_2$ , 400 MHz)  $\delta = 7.84$  (d,  $^3J_{\text{HH}} = 9.1$  Hz, 2H, H3), 6.88 (d,  $^3J_{\text{HH}} = 9.1$  Hz, 2H, H4), 7.38 (t,  $^3J_{\text{HH}} = 8.0$  Hz, 4H, H4'), 7.21 (t,  $^3J_{\text{HH}} = 8.0$  Hz, 2H, H5'), 7.20 (d,  $^3J_{\text{HH}} = 8.0$  Hz, 4H, H3'), 5.02 (q,  $^3J_{\text{HH}} = 7.0$  Hz, 2H,  $\text{H}_{\text{CH}_2}$ ), 1.65 ppm (t,  $^3J_{\text{HH}} = 7.1$  Hz, 3H,  $\text{H}_{\text{CH}_3}$ ).  $^{13}\text{C}$  NMR ( $\text{CD}_2\text{Cl}_2$ , 101 MHz)  $\delta = 305.8$  ( $^1J_{\text{WC}} = \text{n.o.}$ ,  $\text{C}_{\text{carb}}$ ), 203.8 ( $^1J_{\text{WC}} = \text{n.o.}$ ,  $\text{C}_{\text{W}(\text{CO})_5}$ , *trans*), 198.6 ( $^1J_{\text{WC}} = 64.4$  Hz,  $\text{C}_{\text{W}(\text{CO})_5}$ , *cis*), 151.5 (C2), 147.2, 145.5 (C5, C2'), 132.8 (C3), 130.2, 127.0, (C3', C4'), 125.9 (C4), 117.8 (C5'), 79.7 ( $\text{C}_{\text{CH}_2}$ ), 15.2 ppm ( $\text{C}_{\text{CH}_3}$ ). ESI-MS (2.8 V, positive mode,  $m/z$ ): calcd for  $[\text{M} + \text{H}]^+$  626.0800; found 626.0856.

**4a:** The same synthesis procedure as for **1a** was followed. Tris(4-bromophenyl)amine (4.82 g, 10.0 mmol),  $n\text{-BuLi}$  (6.60 mL, 10.0 mmol),  $\text{W}(\text{CO})_6$  (3.52 g, 10.0 mmol),  $\text{Et}_3\text{OBF}_4$  (1.89 g, 10.0 mmol) provided 1.23 g (15.7%) of the product.  $\text{C}_{26}\text{H}_{17}\text{O}_6\text{NBr}_2\text{W}$ .  $^1\text{H}$  NMR ( $\text{CD}_2\text{Cl}_2$ , 300 MHz)  $\delta = 7.80$  (d,  $^3J_{\text{HH}} = 9.0$  Hz, 2H, H3), 7.47 (d,  $^3J_{\text{HH}} = 8.8$  Hz, 4H, H3'), 7.05 (d,  $^3J_{\text{HH}} = 8.8$  Hz, 4H, H4'), 6.94 (d,  $^3J_{\text{HH}} = 9.0$  Hz, 2H, H4), 5.04 (q,  $^3J_{\text{HH}} = 7.0$  Hz, 2H,  $\text{H}_{\text{CH}_2}$ ), 1.67 ppm (t,  $^3J_{\text{HH}} = 7.1$  Hz, 3H,  $\text{H}_{\text{CH}_3}$ ).  $^{13}\text{C}$  NMR ( $\text{CD}_2\text{Cl}_2$ , 75 MHz)  $\delta = 308.4$  ( $^1J_{\text{WC}} = \text{n.o.}$ ,  $\text{C}_{\text{carb}}$ ), 203.4 ( $^1J_{\text{WC}} = \text{n.o.}$ ,  $\text{C}_{\text{W}(\text{CO})_5}$ , *trans*), 197.9 ( $^1J_{\text{WC}} = \text{n.o.}$ ,  $\text{C}_{\text{W}(\text{CO})_5}$ , *cis*), 152.0 (C2), 147.2 (C5), 145.3 (C2'), 132.8 (C3'), 131.6 (C3), 127.6 (C4'), 119.4 (C5'), 118.4 (C4), 80.1 ( $\text{C}_{\text{CH}_2}$ ), 15.2 ppm ( $\text{C}_{\text{CH}_3}$ ). ESI-MS (2.8 V, positive mode,  $m/z$ ): calcd for  $[\text{M}]^+$  782.8966; found 782.9845.

**1b:** Dimethylamine hydrochloride (1.63 g, 20.0 mmol), KOH (1.12 g, 20.0 mmol) and **1a** (0.94 g, 2.1 mmol) were suspended or dissolved in 10 mL of THF. Distilled  $\text{H}_2\text{O}$  was added dropwise until the KOH

had dissolved, upon which the initially orange solution turned bright yellow (instantaneous reaction). The THF was removed under vacuum to form a yellow suspension in the remaining  $\text{H}_2\text{O}$ .  $\text{Et}_2\text{O}$  (15 mL) was added to the reaction vessel, dissolving the yellow product. The organic phase was isolated and washed three times with distilled  $\text{H}_2\text{O}$  saturated with  $\text{NHMe}_2\cdot\text{HCl}$  after which it was dried over  $\text{MgSO}_4$  and filtered. The bright yellow product was isolated by column chromatography using *n*-hexane and  $\text{CH}_2\text{Cl}_2$  as solvents. Yield = 0.77 g (80.2%).  $\text{C}_{14}\text{H}_{11}\text{O}_5\text{NW}$ .  $^1\text{H}$  NMR ( $\text{CD}_2\text{Cl}_2$ , 300 MHz)  $\delta = 7.42$  (dt,  $^3J_{\text{HH}} = 7.8$ ,  $^4J_{\text{HH}} = 1.7$  Hz, 2H, H4), 7.18 (dt,  $^3J_{\text{HH}} = 7.8$ ,  $^4J_{\text{HH}} = 1.4$  Hz, 1H, H5), 6.80 (dd,  $^3J_{\text{HH}} = 7.8$ ,  $^4J_{\text{HH}} = 1.2$  Hz, 2H, H3), 3.93 (s, 3H,  $\text{NMe}$ ), 3.03 ppm (s, 3H,  $\text{NMe}$ ).  $^{13}\text{C}$  NMR ( $\text{CD}_2\text{Cl}_2$ , 75 MHz)  $\delta = 256.7$  ( $^1J_{\text{WC}} = 46.0$  Hz,  $\text{C}_{\text{carb}}$ ), 204.8 ( $^1J_{\text{WC}} = 63.5$  Hz,  $\text{C}_{\text{W}(\text{CO})_5}$ , *cis*), 199.0 ( $^1J_{\text{WC}} = 63.7$  Hz,  $\text{C}_{\text{W}(\text{CO})_5}$ , *trans*), 153.8 (C2), 128.8 (C3), 126.6 (C5), 119.9 (C4), 44.8 ppm ( $\text{NMe}_2$ ).

**2b:** The same synthesis procedure as for **1b** was followed using  $\text{NHMe}_2\cdot\text{HCl}$  (3.26 g, 40.0 mmol), KOH (2.24 g, 40.0 mmol), **2a** (2.09 g, 4.42 mmol). Yield = 1.88 g (85.1%).  $\text{C}_{14}\text{H}_{12}\text{O}_5\text{N}_2\text{W}$ .  $^1\text{H}$  NMR ( $\text{CDCl}_3$ , 400 MHz)  $\delta = 6.74$  (d,  $^3J_{\text{HH}} = 7.1$ , 2H, H3), 6.68 (d,  $^3J_{\text{HH}} = 7.1$  Hz, 2H, H4), 3.89 (s, 3H,  $\text{NMe}$ ), 3.04 (s, 3H,  $\text{NMe}$ ), 2.96 ppm (s, 6H,  $\text{NMe}_2$ ).  $^{13}\text{C}$  NMR ( $\text{CDCl}_3$ , 50 101 MHz)  $\delta = 258.2$  (C1), 205.1 ( $^1J_{\text{WC}} = 63.6$  Hz,  $\text{C}_{\text{W}(\text{CO})_5}$ , *cis*), 199.3 ( $^1J_{\text{WC}} = 63.9$  Hz,  $\text{C}_{\text{W}(\text{CO})_5}$ , *trans*), 149.4 (C2), 143.5 (C5), 122.3, 120.7 (C3), 112.5, 111.3 (C4), 43.8–39.5 ppm (m) ( $\text{NMe}_2$ ).

**3b:** The same synthesis procedure as for **1b** was followed using  $\text{NHMe}_2\cdot\text{HCl}$  (0.33 g, 4.04 mmol), KOH (0.224 g, 4.04 mmol), **3a** (0.253 g, 0.404 mmol). Yield = 0.253 g (100%).  $\text{C}_{26}\text{H}_{20}\text{O}_5\text{N}_2\text{W}$ .  $^1\text{H}$  NMR ( $\text{CD}_2\text{Cl}_2$ , 300 MHz)  $\delta = 7.26$  (t,  $^3J_{\text{HH}} = 8.5$  Hz, 4H, H4'), 7.09 (d,  $^3J_{\text{HH}} = 8.5$  Hz, 4H, H3'), 7.06 (d,  $^3J_{\text{HH}} = 8.6$  Hz, 2H, H3), 7.03 (t,  $^3J_{\text{HH}} = 8.5$  Hz, 2H, H5'), 6.70 (d,  $^3J_{\text{HH}} = 8.6$  Hz, 2H, H4), 3.91 (s, 3H,  $\text{NMe}$ ), 3.14 ppm (s, 3H,  $\text{NMe}$ ).  $^{13}\text{C}$  NMR ( $\text{CD}_2\text{Cl}_2$ , 75 MHz)  $\delta = 257.2$  ( $^1J_{\text{WC}} = 45.9$  Hz,  $\text{C}_{\text{carb}}$ ), 204.9 ( $^1J_{\text{WC}} = 62.9$  Hz,  $\text{C}_{\text{W}(\text{CO})_5}$ , *trans*), 199.1 ( $^1J_{\text{WC}} = 64.1$  Hz,  $\text{C}_{\text{W}(\text{CO})_5}$ , *cis*), 148.8 (C2), 148.1 (C2), 146.3 (C5'), 129.7 (C4'), 124.6 (C3') 124.0 (C5'), 123.4, 121.2 (C3, C4), 44.9 ppm ( $\text{NMe}_2$ ). ESI-MS (2.8 V, positive mode,  $m/z$ ): calcd for  $[\text{M} + \text{H}]^+$  625.0960; found 625.0912.

**4b:** The same synthesis procedure as for **1b** was followed using  $\text{NHMe}_2\cdot\text{HCl}$  (0.49 g, 6.0 mmol), KOH (0.34 g, 6.0 mmol), **4a** (0.481 g, 0.613 mmol). Yield = 0.480 g (100%).  $\text{C}_{26}\text{H}_{18}\text{O}_5\text{N}_2\text{Br}_2\text{W}$ .  $^1\text{H}$  NMR ( $\text{CD}_2\text{Cl}_2$ , 400 MHz)  $\delta = 7.37$  (d,  $^3J_{\text{HH}} = 8.9$  Hz, 4H, H3'), 7.11 (d,  $^3J_{\text{HH}} = 8.8$  Hz, 2H, H3), 6.96 (d,  $^3J_{\text{HH}} = 8.9$  Hz, 4H, H4'), 6.75 (d,  $^3J_{\text{HH}} = 8.8$  Hz, 2H, H4), 3.93 (s, 3H,  $\text{NMe}$ ), 3.16 ppm (s, 3H,  $\text{NMe}$ ).  $^{13}\text{C}$  NMR ( $\text{CD}_2\text{Cl}_2$ , 101 MHz)  $\delta = 256.9$  ( $^1J_{\text{WC}} = \text{n.o.}$ ,  $\text{C}_{\text{carb}}$ ), 204.8 ( $^1J_{\text{WC}} = 63.0$  Hz,  $\text{C}_{\text{W}(\text{CO})_5}$ , *trans*), 199.2 ( $^1J_{\text{WC}} = 62.8$  Hz,  $\text{C}_{\text{W}(\text{CO})_5}$ , *cis*), 149.9 (C2), 146.8 (C2') 145.4 (C5), 132.9 (C3'), 125.9 (C4'), 125.3 (C3), 121.6 (C4), 115.9 (C5'), 54.1, 44.8 ppm ( $\text{NMe}_2$ ).

**2c:** A solution of diethyl ether was saturated with  $\text{NH}_3(\text{g})$  and added to a solution of **2a** (2.87 g, 5.73 mmol) in diethyl ether and allowed to stir for 2 hours. The bright yellow product was isolated by trituration using dichloromethane and *n*-hexane as solvents. The trituration was repeated three times. Yield: 0.766 g (28.3%).  $\text{C}_{14}\text{H}_{12}\text{O}_5\text{N}_2\text{W}$ .  $^1\text{H}$  NMR ( $\text{CDCl}_3$ , 400 MHz)  $\delta = 8.47$  (s, *br*, 1H,  $\text{NH}_2$ ), 8.05 (s, *br*, 1H,  $\text{NH}_2$ ), 7.50 (d,  $^3J_{\text{HH}} = 9.1$  Hz, 2H, H3), 6.68 (d,  $^3J_{\text{HH}} = 9.1$  Hz, 2H, H4), 3.05 ppm (s, 6H,  $\text{NMe}_2$ ).  $^{13}\text{C}$  NMR ( $\text{CDCl}_3$ , 101 MHz)  $\delta = 255.3$  ( $\text{C}_{\text{carb}}$ ), 203.2 ( $^1J_{\text{WC}} = \text{n.o.}$ ,  $\text{C}_{\text{W}(\text{CO})_5}$ , *cis*), 198.9, ( $^1J_{\text{WC}} = 47.1$  Hz,  $\text{C}_{\text{W}(\text{CO})_5}$ , *trans*), 152.8 (C2), 137.6 (C5), 129.0 (C3), 111.2 (C4), 40.1 ppm ( $\text{NMe}_2$ ).

**2c\*:**  $p\text{-}[\{1^6\text{-Me}_2\text{NC}_6\text{H}_4\text{C}(\text{OEt})\text{W}(\text{CO})_3\}\text{Cr}(\text{CO})_3]^{\text{Ba}}$  (0.12 g, 0.19 mmol) was dissolved in diethyl ether.  $\text{NH}_3(\text{g})$ -saturated ether was added to the solution at ambient temperature until a colour change was observed from red/brown to bright yellow. The bright yellow product was isolated by column chromatography using *n*-hexane and  $\text{CH}_2\text{Cl}_2$  as solvents. Yield = 0.101 g (87.4%).  $^1\text{H}$  NMR ( $\text{CDCl}_3$ , 400 MHz)  $\delta = 8.93$  (*br*, s, 1H,  $\text{NH}_2$ ), 8.69 (*br*, s, 1H,  $\text{NH}_2$ ), 5.45 (d,  $^3J_{\text{HH}} =$

7.2 Hz, 2H, H3), 4.74 (d,  $^3J_{\text{HH}}=7.2$  Hz, 2H, H4), 2.95 ppm (s, 6H, NMe<sub>2</sub>). <sup>13</sup>C NMR (CDCl<sub>3</sub>, 101 MHz)  $\delta=261.4$  (C<sub>carb</sub>), 232.9 (Cr(CO)<sub>3</sub>), 203.0 ( $J_{\text{WC}}=n.o.$ , C<sub>W(CO)5</sub>, cis), 197.5, ( $^1J_{\text{WC}}=47.1$  Hz, C<sub>W(CO)5</sub>, trans), n.o. (C2, C5), 93.8, 92.1 (C3), 71.9, 70.1 (C4), 40.5, 39.1 ppm (NMe<sub>2</sub>). Signals of the phenyl carbon atoms are duplicated due to planar chirality.

## Associated Content

Supplementary Information (SI) submitted consists of NMR data, DFT calculations, infrared and spectroelectrochemistry graphs and crystallography data. The Supporting Information is available free of charge. Crystallographic data have been deposited with the Cambridge Crystallographic Data Centre as supplementary publication with deposition numbers CCDC-1917579 for **2a**, CCDC-1917580 for **2b**, CCDC-1925894 for **2c**, CCDC-1925895 for **2c\***, CCDC-1925896 for **3a**. These data can be obtained free of charge via [www.ccdc.cam.ac.uk/data\\_request/cif](http://www.ccdc.cam.ac.uk/data_request/cif), or by emailing [data\\_request@ccdc.cam.ac.uk](mailto:data_request@ccdc.cam.ac.uk), or by contacting The Cambridge Crystallographic Data Centre, 12 Union Road, Cambridge CB2 1EZ, UK; fax: +44 1223 336033.

## Author contributions

The manuscript was written through contributions of all authors. All authors have approved to the final version of the manuscript.

## Acknowledgements

The authors acknowledge support by the state of Baden-Württemberg through bwHPC and the Deutsche Forschungsgemeinschaft (DFG) through grant no INST 40/467-1 FUGG (JUSTUS cluster). In addition, SL and N-a.W. acknowledge the Alexander von Humboldt Foundation and University of Pretoria for funding research visits in Konstanz. SL acknowledges the NRF (RSA) for financial support of the project by GUN 87788 and 95772 grants. N-a.W gratefully acknowledges financial support by the University of Pretoria and the NRF for a research visit to the Universität Konstanz and to Prof. Winter for hosting her on two occasions. Open access funding enabled and organized by Projekt DEAL.

**Keywords:** Fischer carbene complexes · tungsten carbene complexes · (spectro)electrochemistry · quantum chemical calculations

- [1] a) A. Rahm, A. L. Rheingold, W. D. Wulff, *Tetrahedron* **2000**, *56*, 4951–4965; b) H. Rudler, A. Parlier, T. Durand-Reville, B. Martin-Vaca, M. Audouin, E. Garrier, V. Certal, J. Vaissermann, *Tetrahedron* **2000**, *56*, 5001–5027; c) M. Tafipolsky, W. Scherer, K. Öfele, G. Artus, B. Pedersen, W. A. Herrmann, G. S. McGrady, *J. Am. Chem. Soc.* **2002**, *124*, 5865–5880; d) I. Fernández, M. A.

- Sierra, F. P. Cossío, *J. Org. Chem.* **2008**, *73*, 2083–2089; e) A. Collado, M. Gómez-Gallego, A. Santiago, M. A. Sierra, *Eur. J. Org. Chem.* **2019**, *2019*, 369–377; f) P. de Frémont, N. Marion, S. P. Nolan, *Coord. Chem. Rev.* **2009**, *253*, 862–892; g) H. G. Raubenheimer, *Dalton Trans.* **2014**, *43*, 16959–16973.
- [2] a) B. Weyershausen, M. Nieger, K. H. Dötz, *J. Organomet. Chem.* **2000**, *602*, 37–44; b) H. Dialer, K. Polborn, W. Beck, *J. Organomet. Chem.* **1999**, *589*, 21–28; c) M. Salmain, E. Licandro, C. Baldoli, S. Maiorana, H. Tran-Huy, G. Jaouen, *J. Organomet. Chem.* **2001**, *617–618*, 376–382.
- [3] a) D. Bourissou, O. Guerret, F. P. Gabbaï, G. Bertrand, *Chem. Rev.* **2000**, *100*, 39–92; b) R. R. Schrock, *Angew. Chem. Int. Ed.* **2006**, *45*, 3748–3759; *Angew. Chem.* **2006**, *118*, 3832–3844; c) D. Tapu, D. A. Dixon, C. Roe, *Chem. Rev.* **2009**, *109*, 3385–3407.
- [4] O. Schuster, L. Yang, H. G. Raubenheimer, M. Albrecht, *Chem. Rev.* **2009**, *109*, 3445–3478.
- [5] a) H. G. Raubenheimer, S. Cronje, *Dalton Trans.* **2008**, 1265–1272; b) R. Ganesamoorthi, A. Thakur, D. Sharmila, V. Ramkumar, S. Ghosh, *J. Organomet. Chem.* **2013**, *726*, 56–61.
- [6] H. Meerwein, *Org. Synth.* **1966**, *46*, 113–115.
- [7] a) J. T. Guy, D. W. Bennett, *Trans. Met. Chem.* **1984**, *9*, 43–46; b) Z. Lamprecht, S. G. Radhakrishnan, A. Hildebrandt, H. Lang, D. C. Liles, N.-a. Weststrate, S. Lotz, D. I. Bezuidenhout, *Dalton Trans.* **2017**, *46*, 13983–13993.
- [8] a) N.-a. Weststrate, S. Bouwer, C. Hassenrück, N. A. van Jaarsveld, D. C. Liles, R. F. Winter, S. Lotz, *J. Organomet. Chem.* **2018**, *869*, 54–66; b) E. O. Fischer, C. G. Kreiter, H. J. Kollmeier, J. Müller, R. D. Fischer, *J. Organomet. Chem.* **1971**, *28*, 237–258.
- [9] C. F. Bernasconi, M. Ali, *J. Am. Chem. Soc.* **1999**, *121*, 11384–11394.
- [10] C. K. Murray, B. P. Warner, V. Dragisich, W. D. Wulff, R. D. Rogers, *Organometallics* **1990**, *9*, 3142–3151.
- [11] a) R. J. Staples, D. M. Potts, J. C. Yoder, *Z. Kristallogr.* **1995**, *210*, 381–382; b) J. A. Denny, M. Y. Darensbourg, *Coord. Chem. Rev.* **2016**, *324*, 82–89.
- [12] N.-a. Weststrate, I. Fernández, D. C. Liles, N. van Jaarsveld, S. Lotz, *Organometallics* **2015**, *34*, 696–710.
- [13] C. F. Macrae, I. J. Bruno, J. A. Chisholm, P. R. Edgington, P. McCabe, E. Pidcock, L. Rodriguez-Monge, R. Taylor, J. Van De Sreek, P. A. Wood, *J. Appl. Crystallogr.* **2008**, *41*, 466–470.
- [14] a) E. O. Fischer, *Pure Appl. Chem.* **1970**, *24*, 407–423; b) N. Kuhn, T. Kratz, R. Boese, D. Bläser, *J. Organomet. Chem.* **1994**, *470*, C8–C11; c) K. Ulrich, V. Guerschais, K.-H. Dötz, L. Toupet, H. Le Bozec, *Eur. J. Inorg. Chem.* **2001**, 725–732; d) B. van der Westhuizen, J. M. Speck, M. Korb, J. Friedrich, D. I. Bezuidenhout, H. Lang, *Inorg. Chem.* **2013**, *52*, 14253–14263; e) M. Landman, R. Pretorius, R. Fraser, B. E. Buitendach, M. M. Conradie, P. H. van Rooyen, J. Conradie, *Electrochim. Acta* **2014**, *130*, 104–118; f) Z. Lamprecht, M. M. Moeng, D. C. Liles, S. Lotz, D. I. Bezuidenhout, *Polyhedron* **2019**, *158*, 193–207.
- [15] C. P. Casey, T. J. Burkhardt, C. A. Bunnell, J. C. Calabrese, *J. Am. Chem. Soc.* **1977**, *99*, 2127–2134.
- [16] F. E. Hahn, V. Langenhahn, T. Pape, *Chem. Commun.* **2005**, 5390–5392.
- [17] R. Aumann, X. Fu, D. Vogt, R. Fröhlich, O. Kataeva, *Organometallics* **2002**, *21*, 2736–2742.
- [18] A. Schwenger, W. Frey, C. Richert, *Angew. Chem. Int. Ed.* **2016**, *55*, 13706–13709; *Angew. Chem.* **2016**, *128*, 13910–13913.
- [19] A. N. Sobolev, V. K. Belsky, I. P. Romm, N. Y. Chernikova, E. N. Guryanova, *Acta Crystallogr. Sect. C* **1985**, *41*, 967–971.
- [20] a) I. Hoskovcova, J. Rohacova, D. Dvorak, T. Tobrman, S. Zalis, R. Zverinova, J. Ludvik, *Electrochim. Acta* **2010**, *55*, 8341–8351; b) I. Hoskovcova, R. Zverinova, J. Rohacova, D. Dvorak, T. Tobrman, S. Zalis, J. Ludvik, *Electrochim. Acta* **2011**, *56*, 6853–6859; c) H. Kvapilova, I. Hoskovcova, M. Kayanuma, C. Daniel, S.

- Zalis, *J. Phys. Chem. A* **2013**, *117*, 11456–11463; d) H. Kvapilová, I. Hoskovcová, J. Ludvík, S. Záliš, *Organometallics* **2014**, *33*, 4964–4972; e) C. Baldoli, P. Cerea, L. Falciola, C. Giannini, E. Licandro, S. Maiorana, P. Mussini, D. Perdicchia, *J. Organomet. Chem.* **2005**, *690*, 5777–5787; f) M. Landman, R. Pretorius, B. E. Buitendach, P. H. van Rooyen, J. Conradie, *Organometallics* **2013**, *32*, 5491–5503; g) G. K. Ramollo, M. J. López-Gómez, D. C. Liles, L. C. Matsinha, G. S. Smith, D. I. Bezuidenhout, *Organometallics* **2015**, *34*, 5745–5753; h) B. A. Anjali, C. H. Suresh, *New J. Chem.* **2018**, *42*, 18217–18224; i) I. Hoskovcová, J. Ludvík, *Curr. Opin. Electrochem.* **2019**, *15*, 165–174; j) B. van der Westhuizen, P. J. Swarts, L. M. van Jaarsveld, D. C. Liles, U. Siegert, J. C. Swarts, I. Fernández, D. I. Bezuidenhout, *Inorg. Chem.* **2013**, *52*, 6674–6684; k) G. M. Chu, A. Guerrero-Martínez, I. Fernández, M. Á. Sierra, *Chem. Eur. J.* **2014**, *20*, 1367–1375; l) G. M. Chu, I. Fernández, M. A. Sierra, *Chem. Eur. J.* **2013**, *19*, 5899–5908; m) D. I. Bezuidenhout, I. Fernández, B. van der Westhuizen, P. J. Swarts, J. C. Swarts, *Organometallics* **2013**, *32*, 7334–7344; n) G. M. Chu, A. Guerrero-Martínez, C. Ramírez de Arellano, I. Fernández, M. A. Sierra, *Inorg. Chem.* **2016**, *55*, 2737–2747; o) T. Bens, P. Boden, P. Di Martino-Fumo, J. Beerhues, U. Albold, S. Sobottka, N. I. Neuman, M. Gerhards, B. Sarkar, *Inorg. Chem.* **2020**, *59*, 15504–15513.
- [21] a) E. T. Seo, R. F. Nelson, J. M. Fritsch, L. S. Marcoux, D. W. Leedy, R. N. Adams, *J. Am. Chem. Soc.* **1966**, *88*, 3498–3503; b) E. Steckhan, *Angew. Chem. Int. Ed.* **1986**, *25*, 683–701; *Angew. Chem.* **1986**, *98*, 681–699; c) S. Dapperheld, E. Steckhan, K.-H. G. Brinkhaus, T. Esch, *Chem. Ber.* **1991**, *124*, 2557–2567; d) M. G. Vivas, D. L. Silva, J. Malinge, M. Boujtita, R. Zalesny, W. Bartkowiak, H. Ågren, S. Canuto, L. De Boni, E. Ishow, C. R. Mendonca, *Sci. Rep.* **2014**, *4*, 4447.
- [22] a) R. P. Van Duyne, C. N. Reilley, *Anal. Chem.* **1971**, *44*, 158–169; b) H. Debrodt, K. E. Heusler, *Z. Phys. Chem. (Wiesbaden)* **1981**, *125*, 35–48; c) T. Sumiyoshi, *Chem. Lett.* **1995**, 645–646.
- [23] A. J. L. Pombeiro, *J. Organomet. Chem.* **2005**, *690*, 6021–6040.
- [24] I. Hoskovcová, J. Roháčková, L. Meca, T. Tobrman, D. Dvořák, J. Ludvík, *Electrochim. Acta* **2005**, *50*, 4911–4915.
- [25] K. Sreenath, C. V. Suneesh, V. K. Ratheesh Kumar, K. R. Gopidas, *J. Org. Chem.* **2008**, *73*, 3245–3251.
- [26] a) W. Strohmeier, F. J. Müller, *Chem. Ber.* **1967**, *100*, 2812–2821; b) B. Breit, *J. Mol. Catal. A* **1999**, *143*, 143–154.
- [27] a) S. J. Sherlock, D. C. Boyd, B. Moasser, W. L. Gladfelter, *Inorg. Chem.* **1991**, *20*, 3626–3632; b) D. I. Bezuidenhout, B. van der Westhuizen, P. J. Swarts, T. Chatturgoon, O. Q. Munro, I. Fernández, J. C. Swarts, *Chem. Eur. J.* **2014**, *20*, 4974–4985.
- [28] M. Krejčík, M. Danek, F. Hartl, *J. Electroanal. Chem.* **1991**, *317*, 179–187.
- [29] M. J. Frisch, G. W. Trucks, H. B. Schlegel, G. E. Scuseria, M. A. Robb, J. R. Cheeseman, G. Scalmani, V. Barone, G. A. Petersson, H. Nakatsuji, X. Li, M. Caricato, A. Marenich, J. Bloino, B. G. Janesko, R. Gomperts, B. Mennucci, H. P. Hratchian, J. V. Ortiz, A. F. Izmaylov, J. L. Sonnenberg, D. Williams-Young, F. L. F. Ding, F. Egidi, J. Goings, B. Peng, A. Petrone, T. Henderson, D. Ranasinghe, V. G. Zakrzewski, J. Gao, N. Rega, G. Zheng, W. Liang, M. Hada, M. Ehara, K. Toyota, R. Fukuda, J. Hasegawa, M. Ishida, T. Nakajima, Y. Honda, O. Kitao, H. Nakai, T. Vreven, K. Throssell, J. J. A. Montgomery, J. E. Peralta, F. Ogliaro, M. Bearpark, J. J. Heyd, E. Brothers, K. N. Kudin, V. N. Staroverov, T. Keith, R. Kobayashi, J. Normand, K. Raghavachari, A. Rendell, J. C. Burant, S. S. Iyengar, J. Tomasi, M. Cossi, J. M. Millam, M. Klene, C. Adamo, R. Cammi, J. W. Ochterski, R. L. Martin, K. Morokuma, O. Farkas, J. B. Foresman, D. J. Fox, in *Wallingford, CT* (Ed.: G. Inc.), **2016**.
- [30] M. Cossi, N. Rega, G. Scalmani, V. Barone, *J. Comput. Chem.* **2003**, *24*, 669–681.
- [31] a) D. Andrae, U. Haeussermann, M. Dolg, H. Stoll, H. Preuss, *Theor. Chim. Acta* **1990**, *77*, 123–141; b) F. Weigend, R. Ahlrichs, *Phys. Chem. Chem. Phys.* **2005**, *7*, 3297–3305; c) S. H. Vosko, L. Wilk, M. Nusair, *Can. J. Phys.* **1980**, *58*, 1200–1211.
- [32] a) A. D. Becke, *J. Chem. Phys.* **1993**, *98*, 5648–5652; b) C. Lee, W. Yang, R. G. Parr, *Phys. Rev. B* **1988**, *37*, 785–789; c) P. J. Stephens, F. J. Devlin, C. F. Cabalowski, M. J. Frisch, *J. Phys. Chem.* **1994**, *98*, 11623–11627.
- [33] N. M. O'Boyle, A. L. Tenderholt, K. M. Langner, *J. Comput. Chem.* **2008**, *29*, 839–845.
- [34] M. D. Hanwell, D. E. Curtis, D. C. Lonie, T. Vandermeersch, E. Zurek, G. R. Hutchison, *J. Cheminf.* **2012**, *4*, 17.
- [35] O. Tange, *USENIX Magazine* **2011**, *36*, 42–47.
- [36] W. Humphrey, A. Dalke, K. Schulten, *J. Mol. Graphics* **1996**, *14*, 33–38.
- [37] <http://www.povray.org/download/> **2004**.
- [38] a) COLLECT, Data Collection Software, Nonius B.V., Netherlands, **1998**; b) Z. Otwinowski, W. Minor, in *Methods in Enzymology*, Vol. 276, *Macromolecular Crystallography* (Eds.: C. W. Carter, R. M. Sweet), Academic Press, **1997**, pp. 307–326; c) APEX3 (including SAINT and SADABS), Bruker-AXS inc., Madison, WI, USA, **2002**.
- [39] G. M. Sheldrick, *Acta Crystallogr. Sect. A* **2008**, *64*, 112–122.
- [40] G. M. Sheldrick, *Acta Crystallogr. Sect. A* **2015**, *71*, 3–8.
- [41] SADBS 2.10, Bruker AXS Inc., Madison, WI, USA, **2015**.

Manuscript received: March 5, 2021  
 Revised manuscript received: March 25, 2021  
 Accepted manuscript online: April 26, 2021